Anal. Chem. **2006,** *78,* 6928−6935

Optically Trapping Confocal Raman Microscopy of Individual Lipid Vesicles: Kinetics of Phospholipase A_2-Catalyzed Hydrolysis of Phospholipids in the Membrane Bilayer

Daniel P. Cherney, Grant A. Myers, Robert A. Horton, and Joel M. Harris*

Department of Chemistry, University of Utah, 315 South 1400 East, Salt Lake City, Utah 84112-0850

Phospholipase A_2 (PLA_2)-catalyzed hydrolysis at the *sn*-2 position of 1,2-dimyristoyl-*sn*-glycero-3-phosphocholine in optically trapped liposomes is monitored in situ using confocal Raman microscopy. Individual optically trapped liposomes (0.6 μm in diameter) are exposed to PLA_2 isolated from cobra (*Naja naja naja)* venom at varying enzyme concentrations. The relative Raman scattering intensities of C−C stretching vibrations from the trans and gauche conformers of the acyl chains are correlated directly with the extent of hydrolysis, allowing the progress of the reaction to be monitored in situ on a single vesicle. In dilute vesicle dispersions, the technique allows the much higher local concentration of lipid molecules in a single vesicle to be detected free of interferences from the surrounding solution. Observing the local composition of an optically trapped vesicle also allows one to determine whether the products of enzyme-catalyzed hydrolysis remain associated with the vesicle or dissolve into solution. The observed reaction kinetics exhibited a time lag prior to the rapid hydrolysis. The lag time varied inversely with the enzyme concentration, which is consistent with the products of enzyme-catalyzed lipid hydrolysis reaching a critical concentration that allows the enzyme to react at a much faster rate. The turnover rate of membrane-bound enzyme determined by Raman microscopy during the rapid, burst-phase kinetics was 1200 s^{-1}. Based on previous measurements of the equilibrium for PLA_2 binding to lipid membranes, the average number of enzyme molecules responsible for catalyzing the hydrolysis of lipid on a single optically trapped vesicle is quite small, only two PLA_2 molecules at the lowest enzyme concentration studied.

Phospholipase A_2 (PLA_2) is a family of water-soluble enzymes that acts with calcium ion as a cofactor to catalyze the hydrolysis of the ester linkage at the *sn*-2 position of phospholipids. This reaction yields a lysophospholipid and a free fatty acid as the products of the reaction;[1,2] see Figure 1. The fatty acid products

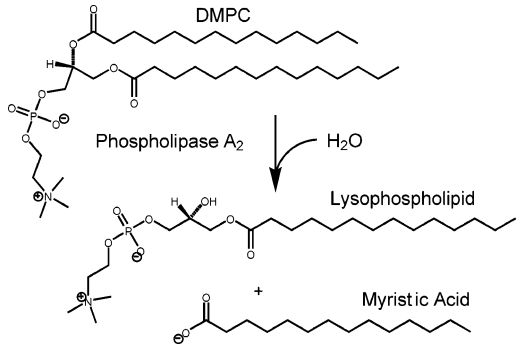

Figure 1. Phospholipase A_2-catalyzed hydrolysis of DMPC.

are bioactive mediators that play roles in cell signaling, inflammation, and allergic reaction while lysophospholipids are powerful detergents that disrupt membrane structure.[3,4] PLA_2 is actually a class of enzymes having similar structures that perform the same function. The different types of phospholipase A_2 are divided into subgroups based on several factors, including amino acid sequence and net charge. These can be found in animal venoms (specifically in bees, lizards, and snakes) and inflammatory cells, as well as pancreatic digestive juices.[2,5−7] Due to the diversity of the function, kinetics, and structure, many phospholipase A_2 enzymes have been studied extensively for the past thirty years.[8−13]

Mechanisms of interfacial catalysis of this enzyme have been discussed in the literature,[13,14] and it is now accepted that the enzyme works in the "scooting" mode, where the enzyme

* To whom correspondence should be addressed. E-mail: harrisj@chem.utah.edu.

(1) Roberts, M. F.; Deems, R. A.; Dennis, E. A. *Proc. Natl. Acad. Sci. U.S.A.* **1977**, *74*, 1950−1954.
(2) Boffa, G. A.; Boffa, M.-C.; Winchenne, J.-J. *Biochim. Biophys. Acta* **1976**, *429*, 828−838.
(3) Gelb, M. H.; Jain, M. K.; Berg, O. G. *FASEB J.* **1994**, *8*, 916−924.
(4) Tatulian, S. A. *Biophys. J.* **2001**, *80*, 789−800.
(5) Nieuwenhuizen, W.; Kunze, H.; de Haas, G. H. *Methods Enzymol.* **1974**, *32B*, 147−154.
(6) Roelofsen, B.; Zwaal, R. F. A.; Woodward, C. B. *Methods Enzymol.* **1974**, *32B*, 131−140.
(7) Dennis, E. A. *J. Biol. Chem.* **1994**, *269*, 13057−13060.
(8) Dupureur, C. M.; Deng, T.; Kwak, J.-G.; Noel, J. P.; Tsai, M.-D. *J. Am. Chem. Soc.* **1990**, *112*, 7074−7076.
(9) Li, Y.; Tsai, M.-D. *J. Am. Chem. Soc.* **1993**, *115*, 8523−8526.
(10) Gelb, M. H.; Jain, M. K.; Hanel, A. M.; Berg, O. G. *Annu. Rev. Biochem.* **1995**, *64*, 653−688.
(11) Raudino, A. *Eur. Phys. J. B* **1998**, *2*, 197−210.
(12) Jain, M. K.; Yu, B.-Z.; Rogers, J.; Gelb, M. H.; Tsai, M.-D.; Hendrickson, E. K.; Hendrickson, H. S. *Biochemistry* **1992**, *31*, 7841−7847.
(13) Jain, M. K.; Gelb, M. H.; Rogers, J.; Berg, O. G. *Methods Enzymol.* **1995**, *249*, 567−614.

10.1021/ac061049b CCC: $33.50
Published on Web 08/30/2006

molecule adheres to a membrane substrate, and the motions of the enzyme and phospholipid molecules in the bilayer or mixed micelle allow hydrolysis of many molecules before the enzyme leaves the membrane or becomes inactive.[13] A result of the scooting mode of activity is that the enzyme shows a preference to hydrolyzing phospholipid molecules at an organized interface over molecules in free solution.[15] It has been found that the enzyme first binds to a membrane substrate and then draws a phospholipid molecule into the catalytic site, as two distinct steps.[16] Knowledge of the structure of different PLA_2s and observation of kinetics via AFM,[17] TEM,[18] fluorescence,[19] and titration techniques[20] have supported this hypothesis.

For a rigorous kinetic description, it is important that adhesion to the lipid bilayer is regarded as a separate step. The overall scheme can be described using the model of Deems et al.[16] as

$$E + A \rightleftharpoons EA \quad (1)$$

$$EA + B \rightleftharpoons EAB \quad (2)$$

$$EAB \rightarrow EA + P \quad (3)$$

where E is the enzyme, A is a binding site on the membrane surface, B is a phospholipid molecule, and P represents the products of the reaction. The first step of the scheme, eq 1, is simply the adsorption of the enzyme to the membrane. This equilibrium is described by the dissociation constant,[16] $K_d = [EA]/[E][A]$, and is reportedly achieved within 1 s.[21] The second step of the kinetic scheme, eq 2, describes the binding of molecules into the active site of the enzyme. The third step of the kinetic scheme, eq 3, describes reaction of substrate molecules to form a product with a rate constant, k_3.

The concentration of enzyme in solution is simple to determine, but the structure of the enzyme and the nature of its binding to a membrane must be known to accurately estimate the number of binding sites on a vesicle, [A], and thus [EAB]. The structures of many different PLA_2 enzymes have been solved by X-ray crystallography.[22] The PLA_2 isoenzymes are relatively small (11−15 kDa) proteins, and their amino acid sequences and folding are responsible for their lipid membrane specificity.[23,24] When a phospholipase A_2 enzyme binds to a substrate, it covers an area of 17.5 nm^2 and excludes water from the space between the enzyme and the substrate molecules.[25] The exclusion of water serves a twofold purpose. First, it maximizes interaction between the enzyme and substrate. Second, it allows the PLA_2 to pull a phospholipid molecule out of the plane of the phospholipid bilayer in order to reach the active site for hydrolysis,[25] reducing interactions between the hydrophobic paraffin chains and water when the phosphatidylcholine molecule is displaced upward from the bilayer. The area covered by the enzyme is equivalent to ∼30 phospholipid molecules, where each phospholipid occupies an area of ∼0.6 nm^2 on the membrane surface.[26,27] The number of binding sites available to the enzyme can be easily estimated with this information.

Cobra (*Naja naja naja*) venom and human group X phospholipase A_2 exhibit stronger binding to zwitterionic than to anionic membranes.[24,28−31] In the present work, *N. naja naja* phospholipase A_2 is introduced into unilamellar liposome samples prepared from a zwitterionic phospholipid, dimyristoylphosphatidylcholine (DMPC), having saturated fatty acid tails that are each 14 carbon atoms long. The gel to liquid-crystalline phase transition temperature of DMPC occurs near 23.5 °C and over a temperature range of ∼1 °C. At the phase transition temperature of the lipid, segregated domains of gel and liquid crystal rafts exist simultaneously,[32] and this coexistence leads to regions of disorder between the phases. Pure phospholipid bilayers have been shown to be poor substrates at temperatures outside the phase transition region[15] due to the lack of structural defects that are starting points for PLA_2-catalyzed hydrolysis. It is currently thought that these regions of membrane disorder between phase domains are where phospholipase A_2 activity begins.[15] The lag in enzyme activity has been observed and attributed to accumulation of hydrolysis products, specifically the lysophospholipid, that perturb the bilayer.[32,33] Experiments have shown that there appears to be a threshold concentration of products that allows the hydrolysis reaction to proceed rapidly in a "burst phase",[33,34] providing there is sufficient phase segregation disorder for initial hydrolysis to occur. Previous measurements of the kinetics of phospholipase A_2 have been successful in obtaining kinetic parameters for activity on populations of lipid micelles[16,35,36] and bilayers.[37−39] Previous studies of DMPC hydrolysis by *N. naja naja* PLA_2 have used lipid micelles (with Triton-X surfactant molecules) as substrates[35,36] where the curvature of the structures reduces the interactions between the hydrophobic lipid tails, analogous to defects in a lipid bilayer.

(14) Berg, O. G.; Gleb, M. H.; Tsai, M.-D.; Jain, M. K. *Chem. Rev.* **2001**, *101*, 2613−2653.
(15) Jain, M. K.; Egmond, M. R.; Verheij, H. M.; Apitz-Castro, R.; Dijkman, R.; de Haas, G. H. *Biochim. Biophys. Acta* **1982**, *688*, 341−348.
(16) Deems, R. A.; Eaton, B. R.; Dennis, E. A. *J. Biol. Chem.* **1975**, *250*, 9013−9020.
(17) Nielsen, L. K.; Balashev, K.; Callisen, T. H.; Bjørnholm, T. *Biophys. J.*, **2002**, *83*, 2617−2624.
(18) Schuster, B.; Gufler, P. C.; Pum, D.; Sleyter, U. B. *Langmuir* **2003**, *19*, 3393−3397.
(19) Grainger, D. W.; Reichart, A.; Ringsdorf, H.; Salesse, C. *Biochim. Biophys. Acta* **1990**, *1023*, 365−379.
(20) Upreti, G. C.; Jain, M. K. *J. Membr. Biol.* **1980**, *55*, 113−121.
(21) Burack, W. R.; Yuan, Q.; Biltonen, R. L. *Biochemistry* **1993**, *32*, 583−589.
(22) Bernstein, F. C.; Koetzle, T. F.; Williams, G. J.; Meyer, E. F., Jr.; Brice, M. D.; Rodgers, J. R.; Kennard, O.; Shimanouchi, T.; Tasumi, M. *J. Mol. Biol.* **1977**, *112*, 535−542.
(23) Deems, R. A.; Dennis, E. A. *J. Biol. Chem.* **1975**, *250*, 9008−9012.
(24) Pan, Y. H.; Yu, B.-Z.; Singer, A. G.; Ghomashchi, F.; Lambeau, G.; Gelb, M. H.; Jain, M. K.; Bahnsom, B. J. *J. Biol. Chem.* **2002**, *277*, 29086−29093.
(25) Jain, M. K.; Vaz, W. L. C. *Biochim. Biophys. Acta* **1987**, *905*, 1−8.
(26) Knoll, W.; Schmidt G.; Rötzer, H.; Henkel, T.; Pfeiffer, W.; Sackmann, E.; Mittler-Neher, S.; Spinke, J. *Chem. Phys. Lipids* **1991**, *57*, 363−374.
(27) Gottlieb, M. H.; Eanes, E. D. *Biophys. J.* **1972**, *12*, 1533−1548.
(28) Ghomashchi, F.; Lin, Y.; Hixon, M. S.; Yu, B.-Z.; Annand, R.; Jain, M. K.; Gelb, M. H. *Biochemistry* **1998**, *37*, 6697−6710.
(29) Reynolds, L. J.; Dennis, E. A. *Methods Enzymol.* **1991**, *197*, 359−365.
(30) Roberts, M. F.; Otnaess, A.-B.; Kensil, C. A.; Dennis, E. A. *J. Biol. Chem.* **1978**, *253*, 1252−1257.
(31) Salach, J. I.; Seng, R.; Tisdale, H.; Singer, T. P. *J. Biol. Chem.* **1971**, *246*, 340−347.
(32) Lee, A. G. *Biochim. Biophys. Acta* **1977**, *472*, 237−281.
(33) Bell, J. D.; Biltonen, R. L. *J. Biol. Chem.* **1992**, *267*, 11046−11056.
(34) Brown, S. D.; Baker, B. L.; Bell, J. D. *Biochim. Biophys. Acta* **1993**, *1168*, 13−22.
(35) Dennis, E. A. *Arch. Biochem. Biophys.* **1973**, *158*, 485−493.
(36) Deems, R. A.; Eaton, B. R.; Dennis, E. A. *J. Biol. Chem.* **1975**, *250*, 9013−9020.
(37) Radvanyi, F.; Jordan, L.; Russo-Marie, F.; Bon, C. *Anal. Biochem.* **1989**, *177*, 103−109.
(38) Kasurinen, J.; Vanha-Perttula, T. *Anal. Biochem.* **1987**, *164*, 96−101.
(39) Elsbach, P.; Weiss, J. *Methods Enzymol.* **1991**, *197*, 24−31.

In this study, time-dependent structural changes in lipid bilayer organization during phospholipase A_2-catalyzed hydrolysis are measured in single, unilamellar DMPC liposomes by Raman microscopy. It was recently demonstrated in our laboratory that it is possible to optically trap single, submicrometer diameter lipid vesicles in the focus of an excitation laser and detect the Raman spectrum of the phospholipid bilayer from a single vesicle over a period of time, with negligible interference from molecules in the surrounding solution.[40] Rather than observing the phospholipase A_2-catalyzed hydrolysis in a bulk sample, it is advantageous to observe the kinetics of phospholipid hydrolysis in the bilayer of a single liposome. The local concentration of lipid molecules is much higher within the femtoliter confocal volume than in a dilute liposome dispersion; lowering the overall concentration of lipid in the sample allows the membrane-bound enzyme concentration to be "buffered" by a much larger concentration in free solution. It is also beneficial to examine a single vesicle when observing transitions in kinetics that depend on the buildup of a critical concentration of products, where the onset of this concentration creates a discrete transition in an individual object whereas the ensemble behavior can be spread out in time. Finally, observing the local composition of an optically trapped vesicle allows one to determine whether the products of enzyme-catalyzed hydrolysis remain associated with the vesicle or dissolve into the surrounding solution.

EXPERIMENTAL SECTION

Reagents and Materials. DMPC was purchased from Avanti Polar Lipids (Alabaster, AL) and dissolved, separately, in chloroform purchased from Sigma (St. Louis, MO). The solutions were used without further purification. An extruder was also purchased from Avanti Polar Lipids. Polycarbonate membranes with a pore size of 0.6 μm were made by Nucleopore (Pleasanton, CA). Tris(hydroxymethyl)aminomethane was purchased from Aldrich (Milwaukee, WI). Calcium chloride was purchased from Fischer (Fair Lawn, NJ), and hydrochloric acid was purchased from Mallinckrodt (Paris, KY). Methanol was purchased from Sigma. All chemicals were used as received. All water used was doubly distilled and then filtered with a Barnstead (Boston, MA) NANOpure II and had a minimum resistivity of 18.2 MΩ·cm. Phospholipase A_2 purified from *N. naja naja* venom was purchased from Sigma as a lyophilized powder. The powder was hydrated with solutions containing 10 mM $CaCl_2$ and 50 mM Tris buffer (pH 8.0). The enzyme solution was stored at −4 °C and warmed to room temperature for at least 30 min prior to use.

Sample Preparation. One milligram of DMPC in chloroform solution was transferred to a 15-mL vial and dried under a stream of nitrogen for 15 min. The resulting film was placed under vacuum for a minimum of 3 h to remove any trace quantities of chloroform. The dried lipid film was hydrated for 1 h above the lipid transition temperature (∼23.5 °C)[41] with 1 mL of an aqueous solution containing 50 mM Tris buffer (pH 8.0) with 10 mM $CaCl_2$ to prepare a 1.5 mM DMPC solution. Approximately 50 μL of the hydrated lipid suspension was extruded 11 times through a polycarbonate membrane with a 0.6-μm pore size to produce unilamellar vesicles; see Supporting Information. Following extrusion, a sample was diluted by a factor of 1/100 with the same buffer solution used for hydrating the lipid, so that the final lipid concentration is [DMPC] = 15 μM. The amount of enzyme in solution for these experiments was either one, two, or three units. Using the activity specified by the supplier, this equated to concentrations of 0.2, 0.4, and 0.6 μg/mL and corresponds to 15, 30, and 45 nM phospholipase A_2 based on a molecular weight of 13 000.[29] Typical *N. naja naja* concentrations reported in the literature for kinetic studies are either on the same order[42,43] or are several orders greater[1,44] than in these experiments.

Confocal Raman Microscopy. The Raman microscope is based on a previous design[45] with minor modifications. Briefly, the 647.1-nm line from a Kr^+ laser (Innova 90, Coherent Inc.) with an output power of 75 mW was sent via a series of mirrors through a band-pass filter (F10-647.1-4, CVI Laser Corp.) and a 4× beam expander (model 50-25-4X-647, Special Optics Inc.) mounted on the back of a Nikon TE 300 inverted fluorescence microscope. The expanded beam was sent through the rear aperture of the microscope, through a another band-pass filter (D647/10, Chroma Tech Inc.) and dichroic beam splitter (655DCLP, Chroma Tech Inc.). The excitation light was then directed through a 100×, 1.4 NA oil immersion microscope objective (CFL PLAN APO, Nikon Inc.) and focused to a 0.60-μm-diameter spot inside the flow cell. The Raman scattering was collected by the same objective and passed through the dichroic beam splitter, a long-pass filter (E660LP, Chroma Tech Inc.), and a holographic notch filter (Kaiser) and focused onto the 50-μm entrance slit of a monochromator (250IS, Chromex Inc.), which defined the confocal volume in the horizontal dimension. A charge-coupled device (CCD) camera (DV420, Andor Inc.) was used to collect the spectrum over a 3-pixel or 66-μm vertical region, which defined the confocal volume in the vertical dimension.

RESULTS AND DISCUSSION

Raman Spectroscopy of DMPC Liposomes. For the Raman spectroscopy analysis of DMPC liposomes, 0.6-μm-diameter liposomes were prepared and diluted into solutions containing varying concentrations of phospholipase A_2. An aliquot of the diluted dispersion was introduced into the flow cell of the microscope, a single vesicle was located and optically trapped, and Raman scattering was collected between 817 and 3220 cm^{-1} with 90-s integrations on the CCD camera. An example Raman spectrum from a single DMPC liposome is plotted in Figure 2, and the observed Raman scattering frequencies from the phosphatidylcholine membrane agree with previous studies and spectral assignments.[46−49] The Raman spectra of various phospholipids are unique for each type of molecule and reflect important aspects of the molecular structure. For example, the degree of order in the acyl chains of the molecules is evident by

(40) Cherney, D. P.; Conboy, J. C.; Harris, J. M. *Anal. Chem.* **2003**, *75*, 6621−6628.
(41) Gugliotti, M.; Politi, M. J.; Chaimovich, H. *J. Colloid Interface Sci.* **1998**, *198*, 1−5.
(42) Kensil, C. R.; Dennis, E. A. *Lipids* **1985**, *20*, 80−83.
(43) Adamich, M.; Dennis, E. A. *J. Biol. Chem.* **1978**, *253*, 5121−5125.
(44) Roberts, M. F.; Deems, R. A.; Dennis, E. A. *J. Biol. Chem.* **1977**, *252*, 6011−6017.
(45) Houlne, M. P.; Sjostrom, C. M.; Uibel, R. H.; Kleimeyer, J. A.; Harris, J. M. *Anal. Chem.* **2002**, *74*, 4311−4319.
(46) Gaber, B. P.; Peticolas, W. L. *Biochim. Biophys. Acta* **1977**, *465*, 260−274.
(47) Brown, K. G.; Peticolas, W. L.; Brown, E. *Biochem. Biophys. Res. Commun.* **1973**, *54*, 358−364.
(48) Litman, B. J.; Lewis, E. N.; Levin, I. W. *Biochemistry* **1991**, *30*, 313−319.
(49) Spiker Jr., R. C.; Levin, I. W. *Biochim. Biophys. Acta* **1975**, *388*, 361−373.

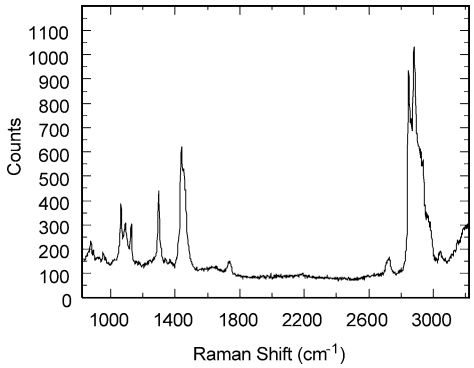

Figure 2. Example Raman spectrum of DMPC over the wavenumber range studied.

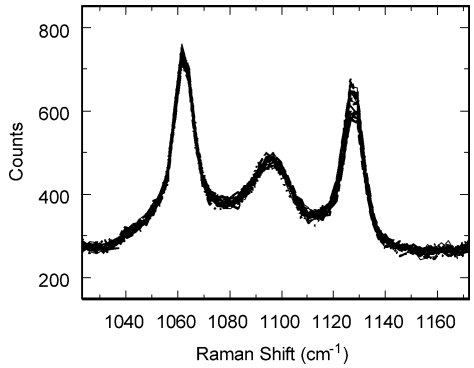

Figure 3. Raman scattering C−C stretching region from optically trapped liposomes exposed to 45 nM PLA_2 at 22 °C, a temperature below the gel to liquid-crystal phase transition temperature of DMPC, ~23.5 °C. No significant change was detectable in any region of these spectra.

observing the relative intensity of the trans 1126-cm^{-1} and gauche 1083-cm^{-1} bands in the C−C stretching region. The relative trans-to-gauche intensity is a sensitive measure of membrane order,[50,51] which should be disrupted by the hydrolysis of the phospholipid and the accumulation of lysophospholipid into the membrane.

First, control samples were analyzed to ensure that no changes in the Raman spectra occur as a result of optical trapping. Since optical forces act on phospholipid molecules in a laser trap, it is necessary to rule these forces out as a cause of any changes in the Raman spectra of DMPC liposomes over time. To confirm that optical forces or other perturbations were not causing any changes, control spectra were taken under identical experimental conditions as the hydrolysis studies except that phospholipase A_2 was omitted from the liposome suspension. Spectra of single, optically trapped liposomes were collected continuously for 60 min with each individual acquisition being integrated for 90 s. There was a slight rise (~6%) in the relative trans intensity during the first 8 min of the run, followed by no subsequent change in the ratio for the remainder of the hour (data not shown).

As a test for the temperature dependence on phospholipase A_2 activity on a DMPC bilayer, the kinetic study was also performed outside the transition temperature region of the lipid. Liposome suspensions were exposed to 15, 30, and 45 nM phospholipase A_2 at temperatures below (22 °C) and above (25 °C) the transition temperature of the lipid (~23.5 °C). At these temperatures, the DMPC should be almost entirely in the gel or liquid-crystalline phase, respectively. After 90 min of exposure to the enzyme, samples at neither temperature exhibited any detectable changes in Raman spectra indicative of hydrolysis. The C−C stretching region is isolated in Figure 3 to show no significant changes in the Raman spectra at a temperature below the transition region; a plot of the relative trans intensity shows a slow 2% drop over 1 h, comparable to the short-term variation in the data. This result confirms that, in the absence of defects in the membrane at phase boundaries, phospholipase A_2-catalyzed hydrolysis is slow.[52]

Enzyme Kinetics at the Membrane Phase Transition Temperature. When Raman spectra were acquired in the phase transition temperature region of DMPC (23.5 °C) in the presence of phospholipase A_2 in solution, significant time-dependent changes

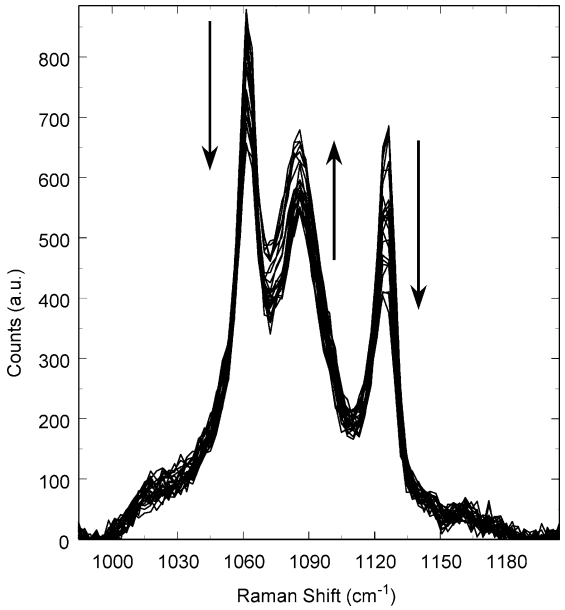

Figure 4. Raman scattering from C−C stretching region from DMPC and its hydrolysis products over 75 min. Spectra are acquired every 90 s; every other spectrum is plotted in this figure. Arrows note the time-dependent trend of the peaks.

were observed in three regions of the spectrum: in the C−C stretching (1050−1140 cm^{-1}), CH_2 bending (1420−1500 cm^{-1}), and CH stretching (2800−2950 cm^{-1}) regions. Changes were expected in the carbonyl peak (1730 cm^{-1}) of the Raman spectrum as well, although due to its weak Raman scattering, no systematic variation in this band could be observed over the noise level. While the trends in all three regions of the spectrum were similar, the C−C stretching region provides the clearest evidence of membrane structural changes that accompany phospholipid hydrolysis; a plot of the intensity changes in this region is shown in Figure 4 for hydrolysis catalyzed by 15 nM phospholipase A_2, where the two peaks associated with trans conformations of the acyl chains decrease during hydrolysis, while the intensity from gauche defects grows. The intensity of Raman scattering from trans conformers at 1126 cm^{-1} (well removed from other bands) is reported as a fraction relative to the total signal from the trans and gauche bands at 1126 and 1083 cm^{-1}, respectively (see Figure 5). Ratio corrections for any variations in collection efficiency over

(50) Yellin, N.; Levin, I. W. *Biochim. Biophys. Acta* **1977**, *489*, 177−190.
(51) Spiker Jr., R. C.; Levin, I. W. *Biochim. Biophys. Acta* **1976**, *433*, 457−468.
(52) Verger, R.; Mieras, M. C. E.; de Haas, G. H. *J. Biol. Chem.* **1973**, *248*, 4023−4034.

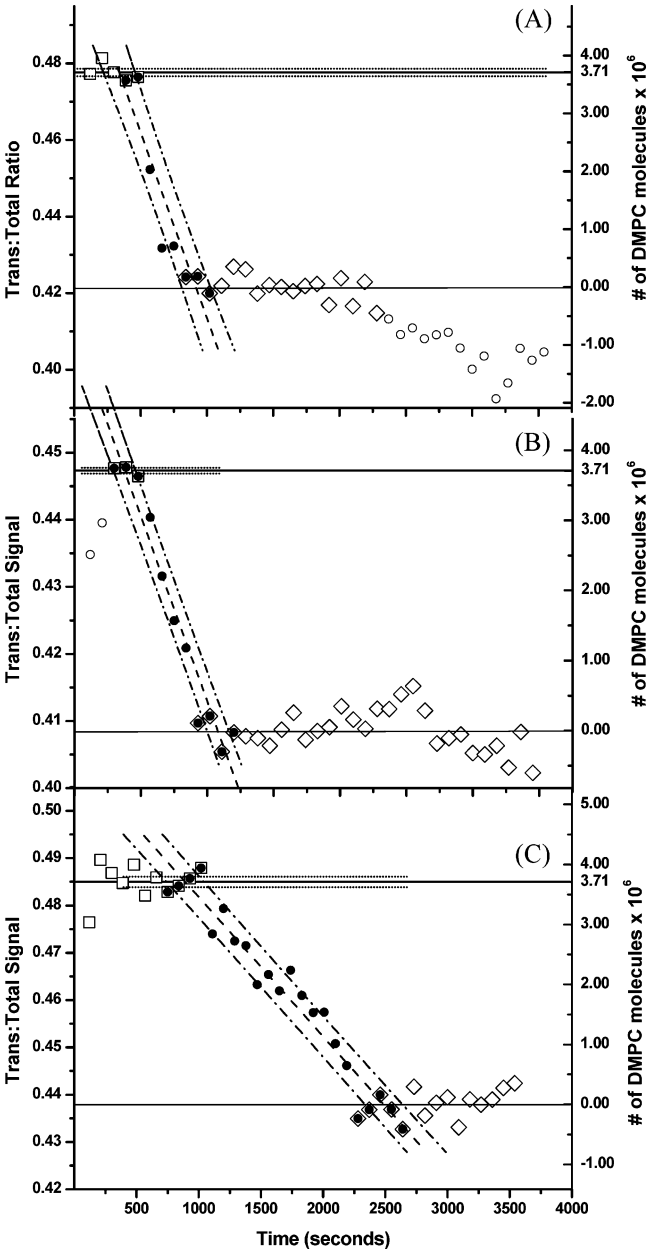

Figure 5. Plots of the reaction time course for a single vesicle at three concentrations of enzyme: 45 (A), 30 (B), and 15 nM (C). The ratio of the C−C trans to total signal is plotted as a function of time after addition of enzyme. On the right-hand *y*-axis, the data are scaled so that the average of the indicated maximum points (□) is set to the number of molecules in a single vesicle, n_s (3.7×10^6), and the average of the indicated minimum points (◇) is set to zero (where the points (○) are not included in that average). Least-squares fits (- -) of the reaction rate are calculated for the indicated points (●), as well as the confidence bands of the fits (- · − and ···) in order to determine the lag time and the error of the lag time.

the course of the experiment and a decrease in the relative trans-band intensity during the reaction indicate the loss of order in the hydrophobic chains of the phospholipid bilayer.[40]

The hydrolysis reaction produces a lysophospholipid and a free fatty acid (see Figure 1); the latter could either remain in the membrane or desorb into the solution because the concentration of lipid is well below the critical micelle concentration of myristic acid (~90 mM).[53] The Raman scattering data indicate desorption of the fatty acid product from the vesicle over the time scale of the hydrolysis reaction is negligible. The total Raman scattering intensities in the C−C stretching, CH_2 bending, and C−H stretching regions do not show a decrease with time, indicating that a vesicle structure remains in the optical trap and the total amount of hydrocarbon in the vesicle does not change significantly over the course of the reaction. The fatty acid product in the lipid bilayer would disrupt chain packing and increase the number of gauche defects in the acyl chains of the remaining DMPC molecules in the trapped sample. In addition, the single acyl chains of the lysophospholipid product do not pack as tightly as intact DMPC, because the headgroup area is not significantly changed by removal of one of the acyl chains; gauche defects in the remaining hydrocarbon chain would allow the space below the headgroup to be filled.

The kinetics of the structural changes were analyzed by calculating the ratio of trans intensity to the total signal from the trans and gauche peaks. A plot of this ratio over time for each concentration of enzyme is shown in Figure 5. It is easily seen from Figure 5 that the rate of change in the membrane structure increases, as expected, with the concentration of phospholipase A_2 used in the reaction. The kinetics show an induction period or "lag phase" that is shorter at higher enzyme concentrations, indicating that the time required for defects to be produced in the bilayer is reduced by the presence of more enzyme that catalyzes the slow hydrolysis of the ordered bilayer. A distinct transition to a rapid rate of reaction or "burst phase" is observed following the induction period, and the rate of rapid reaction also increases with enzyme concentration.

The time dependence of the changes in membrane structure during the course of the reaction can be used to estimate the rate of enzyme-catalyzed hydrolysis. Kinetic parameters for the hydrolysis can be obtained with two approximations being made. The first approximation used in the analysis is that the first step in the kinetic scheme, binding of the enzyme to vesicle membranes ($E + A \rightleftharpoons EA$), reaches equilibrium quickly so that [EA] is constant over the duration of the experiment. This equilibrium has been reported to be attained in less than 1 s,[21] far less time than that required to locate and trap a vesicle in the flow cell. The concentration of EA can be estimated (see below) using a literature value for the equilibrium dissociation constant determined from PLA_2 binding to lipid micelles, $K_d = 5 \times 10^{-4}$ M.[16] The second approximation is that the initial vesicle is composed entirely of intact DMPC molecules, while the final condition corresponds to a vesicle in which all the DMPC molecules in the membrane have been hydrolyzed by the enzyme. This approximation is based on results of a recent electrospray ionization mass spectrometry analysis of the lipid composition of a DMPC vesicle dispersion reacted under identical, PLA_2-catalyzed conditions.[54] The initial vesicle composition is dominated by DMPC, and the hydrolysis kinetics showed lag burst behavior with a very similar time dependence as the Raman microscopy results. Furthermore, the entire DMPC concentration was hydrolyzed by the end of the burst phase of the reaction, where only lysophospholipid and no intact DMPC could be detected.[54] These ESI-MS results imply

(53) Lide, D. R., Ed. *Handbook of Chemistry and Physics*; CRC Press: Boca Raton, FL, 1993.

(54) Myers, G. A.; Fox, C. B.; Cherney, D. P.; Rachlin, E.; Harris, J. M. Monitoring of Phospholipase A2-Catalyzed Lipid Hydrolysis Kinetics Using Electrospray-Ionization Mass Spectrometry. Manuscript in preparation for *J. Lipids Res.*

that either the enzyme migrates to the inner leaflet of the bilayer, which is doubtful due to its size and hydrophilicity, or more likely, rapid lipid flip-flop kinetics at the membrane transition temperature[55,56] eventually bring all of the DMPC to the outer leaflet of the vesicle membrane for reaction.

Following an induction period, the rapid reaction (burst-phase) kinetics appear to be linear for all the concentrations studied. The linearity of this region indicates that the hydrolysis reaction is a zero-order kinetic process,[14] meaning that there is no significant dependence on the remaining concentration of substrate molecules in the bilayer until the reaction is nearly complete. The lack of a substrate concentration dependence to the rate implies that a substrate molecule is always present in the active site of the enzyme so the equilibrium, EA + B ⇌ EAB, is shifted well to the right during burst phase of the reaction. This conclusion means that the rate-limiting step during this phase is the hydrolysis reaction, where the transport of phospholipid substrate molecules to the enzyme and their binding into the active site are fast compared to the rate of reaction. The observed rate of substrate conversion, therefore, depends primarily on the rate, k_3, of the hydrolysis step (EAB → EA + P). The velocity of the overall reaction is $v = \mathrm{d[P]}/\mathrm{d}t = k_3\,[\mathrm{EAB}]$, where [EAB] ≈ [EA], which is the concentration of membrane-bound enzyme molecules in the sample.

The reaction velocity can be determined from the slopes of the burst-phase kinetics observed in the Raman scattering response, scaled to the number of DMPC molecules in a trapped vesicle. The DMPC liposomes prepared in 10 mM $CaCl_2$ were ~0.6 μm in diameter and predominantly (>80%) unilamellar or single bilayer, based on reactive fluorescence quenching experiments; see Supporting Information. From the total surface area of a liposome (including both inner and outer leaflets of the bilayer, 2.2×10^6 nm^2) divided by the mean headgroup area of a phospholipid molecule,[26,27] 0.6 nm^2, the number of DMPC substrate molecules per vesicle is estimated to be $n_s \sim 3.7 \times 10^6$. This value is used to scale the observed spectral changes in a single vesicle, as shown on the right-hand axis of the plots in Figure 5. The slopes of the linear regions of these plots represent the reaction velocity of a single vesicle,

$$-\mathrm{d}n_s/\mathrm{d}t = k_3 n_{EA} \qquad (4)$$

where k_3 is the turnover rate of an enzyme molecule and n_{EA} is the average number of enzyme molecules bound to a vesicle. The single-vesicle reaction velocities, thus defined, are determined from the slopes of the burst-phase kinetic regions of the data in Figure 5. These reaction velocities are plotted in Figure 6 versus the enzyme concentration in solution, [E]. Within the uncertainties of the measured rates, the velocities increase linearly with increasing [E]; this trend would be expected because the average number of membrane-bound enzyme molecules on a vesicle, n_{EA}, should be proportional to the enzyme concentration in solution.

To interpret the kinetic results, the concentration of phospholipase A_2 molecules bound to vesicles, [EA], is determined from the dissociation equilibrium, $K_d = [\mathrm{E}][\mathrm{A}]/[\mathrm{EA}]$, where the concentration of binding sites, [A], is estimated from the concentration of vesicles in solution and their surface area relative to that of the bound enzyme. The concentration of vesicles in solution is [V] ~ 4.0×10^{-12} M, calculated from the concentration of lipid divided by the number of DMPC molecules per vesicle ($n_s \sim 3.7 \times 10^6$; see above). The concentration of binding sites, [A], therefore, can then be estimated from the concentration of vesicles times the vesicle outer surface area (1.1×10^6 nm^2) divided by the area occupied by a bound enzyme[25] (~17.5 nm^2), where [A] ~ 2.6×10^{-7} M. Only the outer surface area of the vesicle is used for estimating the binding site concentration because the enzyme should be too large and hydrophilic to pass through the membrane. The concentration of bound enzyme, [EA], is then determined from the dissociation equilibrium, using a literature value[16] for $K_d = 5 \times 10^{-4}$ M, the concentration of enzyme in solution, and the concentration of binding sites. The bound enzyme concentration, $[\mathrm{EA}] = [\mathrm{E}][\mathrm{A}]/K_d$, is a small fraction of the total enzyme in solution, where [EA] ranged from 7.8 to 23 pM while [E] was varied from 15 to 45 nM in these experiments. Because of the low concentration of vesicles required for an optical trapping experiment, the solution concentration of enzyme, [E], is not significantly altered by the small fraction that binds to vesicle membranes.

To estimate the enzyme turnover rate from the single-vesicle reaction velocities in Figure 6, the values of the concentration of vesicle-bound enzyme in the sample, [EA], must be converted to the number of enzyme molecules per vesicle, n_{EA}, to evaluate k_3 using eq 4. This is a simple conversion because the number of enzyme molecules per vesicle is the ratio of the vesicle-bound enzyme concentration in the solution to the vesicle concentration: $n_{EA} = [\mathrm{EA}]/[\mathrm{V}]$. Using this conversion, the number of enzyme molecules per vesicle, n_{EA}, is plotted as an upper x-axis in Figure 6; remarkably, the number of enzyme molecules

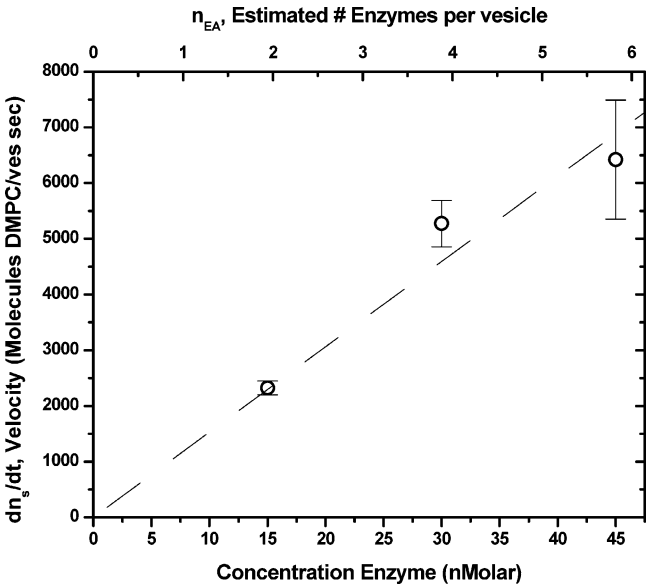

Figure 6. Plot of the reaction velocity (molecules of DMPC hydrolyzed per second, $\mathrm{d}n_s/\mathrm{d}t$) versus enzyme concentration as calculated from the least-squares fits of the bursting-phase points in Figure 5. For a each enzyme concentration, the number of enzyme molecules per vesicle, n_{EA}, is estimated and indicated on the upper x-axis. The slope of the data relative to the upper x-axis corresponds to the enzyme turnover rate.

(55) Liu, J.; Conboy, J. C., *J. Am. Chem. Soc.* **2004**, *126*, 8376−8377.
(56) Liu, J.; Conboy, J. C. *Biophys. J.* **2005**, *89*, 2522−2532.

responsible for the catalyzed hydrolysis reaction on a given vesicle is quite small, where $n_{EA} \sim 2$ PLA_2 molecules per vesicle at a 15 nM enzyme concentration. The slope of the fitted line through the points based on the upper *x*-axis is the substrate turnover rate per enzyme molecule, $k_3 = 1.2\ (\pm\ 0.1) \times 10^3\ s^{-1}$. Given the molecular weight of phospholipase A_2, 13 000,[29] this maximum rate of enzyme turnover (molecules hydrolyzed per enzyme molecule per second) can be converted to more conventional measures of activity, 5.5×10^3 μmol min^{-1} mg of $protein^{-1}$; this result is very close to the value, 4×10^3 μmol min^{-1} mg of $protein^{-1}$, previously reported in a study of *N. naja naja* PLA_2 reactivity on a lipid micelle substrate.[16] The agreement between results indicates that the enzyme reactivity on the lipid micelle, containing Triton-X surfactant molecules, is very close to that observed on a pure lipid vesicle after the buildup of lysophospholipid and fatty acid, which also exhibit surfactant properties.

Prior to the onset of rapid hydrolysis, a lag time was observed to occur where little change in membrane order was observed in the Raman scattering data. The magnitudes of the lag times observed are similar to those reported previously in the literature[33] and also to those observed in ex situ ESI-MS analysis of the lipid composition under identical conditions.[54] This lag time has been attributed to a threshold concentration of lysophospholipid needed in the membrane before rapid (burst-phase) hydrolysis is observed.[33,34,57] The lag time should reflect the amount of time required to produce this critical concentration of lysophospholipid (and fatty acid) molecules by slow hydrolysis of the pure DMPC membrane. The sharp transition to rapid, burst-phase kinetics observed in these single-vesicle data supports the notion that a critical product concentration leads to a significant acceleration in the reaction rate of the enzyme. Despite the much slower reaction prior to this transition, the slow rate should also be proportional to the bound enzyme concentration, [EA], which depends on the concentration of enzyme in solution. The time required to produce a critical concentration of lysophospholipid and fatty acid in the membrane should vary inversely with the reaction rate, where the inverse of the lag time would be proportional to the enzyme concentration. A plot of the inverse of the lag time versus enzyme concentration is shown in Figure 7, where, within the uncertainty in the results, a linear dependence on the PLA_2 concentration is observed. This result shows that the lag time depends on a kinetic step that speeds up in the presence of more enzyme in the sample and is likely due to slow lipid hydrolysis producing membrane defects that eventually accelerate the rate of reaction.

Discussion. The kinetics of phospholipase A_2-catalyzed hydrolysis of individual, optically trapped unilamellar DMPC vesicles has been studied by confocal Raman microscopy. The relative Raman scattering intensities of trans- and gauche-C−C stretching vibrations of the acyl chains could be correlated with the extent of hydrolysis, allowing the progress of the reaction to be monitored in situ on a single vesicle. The observed reaction kinetics exhibited a time lag followed by a burst phase, similar to behavior previously reported in the literature. The turnover rate of membrane-bound enzyme determined by Raman spectroscopy

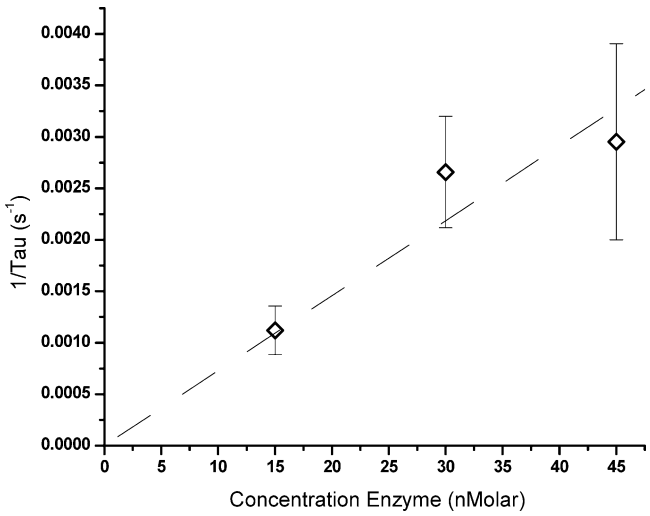

Figure 7. Inverse lag time of the reaction plotted versus enzyme concentration, as calculated from the intersection of the linear least-squares fit and the average of the maximum points indicated in Figure 5. The error bars represent the error estimated from the intersection of the confidence bands of the least-squares fit with the confidence bands of the average of the maximum points, as shown in Figure 5.

during the rapid, burst phase was 1200 s^{-1}. Remarkably, the reaction that is responsible for the complete hydrolysis of the lipid within 20 min was catalyzed by an average of only 2 PLA_2 molecules/vesicle at the lowest enzyme concentration studied. Given this small number of enzyme molecules, one might expect to observe stochastic behavior in the reaction rate at a single vesicle, as the number of enzyme molecules varies due to Poisson statistical fluctuations about this small average number. There is no evidence of stochastic reaction kinetics in the data, however, and this is probably due to the relatively small binding affinity of the enzyme for the membrane. Given the dissociation constant, $K_d = 5 \times 10^{-4}$ M,[16] one would expect rapid exchange between enzyme in solution and on the membrane surface. Even if the rate constant for enzyme binding to the lipid bilayer from solution were 3 orders of magnitude slower than diffusion control, $k_{bind} \sim 10^5\ M^{-1}\ s^{-1}$, the dissociation rate would still be relatively fast, $k_d \sim 50\ s^{-1}$. This estimate suggests that enzyme exchanges on the time scale of tens of milliseconds or less, consistent with the observation that the enzyme binding equilibrium is established in less than 1 s.[21] For the Raman scattering experiments, the observation time for each data point is 90 s, during which the enzyme molecules on the membrane would exchange hundreds or thousands of times, averaging out fluctuations in the small number of molecules catalyzing the reaction. Therefore, while the reaction on a single vesicle is catalyzed by a small number of enzyme molecules on average, the actual number of enzymes participating over the course of the reaction is much greater, due to rapid exchange with the larger population of enzyme molecules in free solution. This time averaging due to fast exchange leads to kinetics that are ergodic, in which observations of a single vesicle reflect the ensemble behavior of the larger dispersion, where ESI-MS data on the vesicle dispersion[54] show reaction kinetics very similar to the Raman microscopy results. Finally, the lag time prior to the rapid hydrolysis reaction was found to vary inversely with the enzyme concentration. This result suggests

(57) Apitz-Castro, R.; Jain, M. K.; de Haas, G. H. *Biochim. Biophys. Acta* **1982**, *688*, 349−356.

that onset of rapid reaction depends on an initially slow, enzyme-catalyzed lipid hydrolysis, which produces defects in the membrane that reach a critical concentration, where the enzyme can react at a much faster rate.

ACKNOWLEDGMENT

This research was supported in part by the National Science Foundation under Grant CHE-0137569. We thank Mahendra Jain of the University of Delaware for suggesting that we try this experiment. Christopher Fox is gratefully acknowledged for helpful discussions.

SUPPORTING INFORMATION AVAILABLE

Additional information as noted in text. This material is available free of charge via the Internet at http://pubs.acs.org.

Received for review June 8, 2006. Accepted July 26, 2006.

AC061049B